

PHOTOSPHERIC AND CHROMOSPHERIC ACTIVE REGIONS IN FOUR YOUNG SOLAR-TYPE STARS¹

K. BIAZZO AND A. FRASCA

INAF–Catania Astrophysical Observatory, Catania, Italy; kbiazzo@oact.inaf.it, afr@oact.inaf.it

G. W. HENRY

Center of Excellence in Information Systems, Tennessee State University, Nashville, TN

AND

S. CATALANO AND E. MARILLI

INAF–Catania Astrophysical Observatory, Catania, Italy

Received 2006 June 23; accepted 2006 October 17

ABSTRACT

We present a photometric and spectroscopic study of four G–K dwarfs, namely HD 166, ϵ Eri, χ^1 Ori, and κ^1 Cet. In three cases, we find a clear spatial association between photospheric and chromospheric active regions. For χ^1 Ori we do not find appreciable variations of photospheric temperature or chromospheric H α emission. We applied a spot/plage model to the observed rotational modulation of temperature and flux to derive spot/plage parameters and to reconstruct a rough “three-dimensional” map of the outer atmosphere of κ^1 Cet, HD 166, and ϵ Eri.

Subject headings: stars: activity — stars: late-type — techniques: photometric — techniques: spectroscopic

1. INTRODUCTION

The atmospheres of main-sequence (MS) stars with spectral types later than F5 exhibit the effects of magnetic activity. At ages of a few hundred Myr, MS stars have magnetic activity levels higher than the Sun but considerably lower than what is typically observed in close binary RS CVn systems or in BY Dra stars. Systematic photometric monitoring of MS FGK stars has been pursued for more than three decades to study starspots in these stars (see, e.g., Radick et al. 1983, 1998; Lockwood et al. 1997; Henry 1999). In particular, Radick et al. (1983) reported that 2 out of 11 stars monitored in Strömgren *uvby* passbands showed light variations anticorrelated with the contemporaneous Ca II H and K S-index. Lockwood et al. (1997) found small-amplitude variations in *b* and *y* filters for about 10 of 41 stars monitored for 11 yr in their Lowell Observatory program and reported photometric variability correlated with mean chromospheric activity. In a more recent paper, Radick et al. (1998) analyzed the same data set and found short-term variability due to rotational modulation in at least 15 of the solar-like stars in their sample.

Recently, several studies have been conducted to analyze the photospheric and chromospheric active regions in young stars (Strassmeier et al. 1993; Stout-Batalha & Vogt 1999), but all the objects studied in these works are ultrafast rotators (UFRs) or pre-main-sequence (PMS) stars. In particular, Strassmeier et al. (1993) found a marginal correlation between the starspot distribution and chromospheric inhomogeneities in LQ Hya, a rapidly rotating ($P_{\text{rot}} \simeq 1.6$ days) single K2 V star, probably just arriving on the zero-age main sequence (ZAMS). However, they could not discriminate between plages and local velocity fields as the cause of the observed variations in the full width at half-maximum (FWHM) of the H α line. On the other hand, the two very active rapidly rotating Pleiades stars, HII 686 and HII 3163, studied by Stout-Batalha & Vogt (1999) did not display the maximum of H α and Ca II infrared triplet (IRT) emission at the same phase of the spot transit. A rotational modulation of the H α emission

with maximum nearly coincident with the minimum of the light curve has been detected by Frasca et al. (1997) in the active rapidly rotating binary TZ CrB. Recently, Frasca et al. (2000) presented the first photospheric/chromospheric study of HD 206860, a solar-type star with an activity level intermediate between the Sun and very active PMS and UFR stars; they used Ca II H and K and H α lines as chromospheric indicators and photometric observations as a photospheric indicator. They found a clear rotational modulation in all the chromospheric and photospheric indicators, proving the presence of an uneven distribution of long-lived active regions and a spatial association between photospheric spots and chromospheric plages, as displayed in the Sun and in the most active RS CVn systems.

In this paper, we study the photospheric and chromospheric surface inhomogeneities in four young MS stars with activity levels intermediate between the Sun and the very active UFR stars. We use light curves and/or temperature measurements as diagnostics of photospheric inhomogeneities and the H α and He I D₃ lines as chromospheric diagnostics. Only for κ^1 Cet, for which we obtained contemporaneous photometric and temperature rotational modulations, are we able to determine a unique solution for the spot parameters (area and temperature) following the method described in Frasca et al. (2005); for χ^1 Ori, the very low amplitude of both light and temperature curves prevented us from applying the spot model; for the last two stars, for which we have only temperature curves, we give only a rough estimate of these spot parameters. Moreover, we apply a spot/plage model to the photospheric and chromospheric rotational modulations in order to investigate the degree of spot/plage association in these mildly active stars, comparing the results with previous results obtained for very active binaries (Frasca & Catalano 1994; Frasca et al. 2005) and single stars (Frasca et al. 2000).

2. OBSERVATIONS

2.1. Target Stars

We selected four early G to early K MS stars to be observed spectroscopically. We also have contemporaneous photometry for two of the stars (κ^1 Cet and χ^1 Ori). The other two stars

¹ Based on observations collected at the Osservatorio Astrofisico di Catania (Italy) and Fairborn Observatory (USA).

TABLE 1
STELLAR SAMPLE

HD Number	Name	$B-V$ (mag)	Spectral Type	P_{rot} (days)	$v \sin i$ (km s ⁻¹)	Companion Stars	Spectral Templates	i^a (deg)
166.....	...	0.747 ^b	K0 V	6.23 ^c	4.1 ^c	...	τ Cet	34
20630.....	κ^1 Cet	0.680 ^b	G5 V	9.20 ^c	4.5 ^c	HD 21585	51 Peg	55
22049.....	ϵ Eri	0.88 ^d	K2 V	11.68 ^e	1.7 ^f	...	54 Psc	30
39587.....	χ^1 Ori	0.59 ^d	G0 V	5.24 ^g	8.6 ^h	HD 37147	10 Tau	65

REFERENCES.— (a) This work; (b) Gonzalez & Piche (1992); (c) Gaidos et al. (2000); (d) Johnson et al. (1966); (e) Donahue et al. (1996); (f) Saar & Osten (1997); (g) Messina et al. (2001); (h) Fekel (1997).

(HD 166 and ϵ Eri) lack contemporaneous photometry. All four stars are listed by HD number in Table 1, along with each star’s name, $B - V$ color index, spectral type, P_{rot} , $v \sin i$, photometric comparison star (for the two stars observed photometrically), the stellar templates we used for spectral subtraction, and the inclination of the rotation axis with respect to line of sight.

A summary of spectroscopic and photometric observations is listed in Table 2.

2.2. Photometry

The photometric observations of κ^1 Cet and χ^1 Ori were acquired with the T4 0.75 m Automatic Photoelectric Telescope (APT) at Fairborn Observatory in southern Arizona (USA). The APT is equipped with an EMI 9124QB photomultiplier detector that measures stars sequentially through Strömgren b and y filters. The observations are reduced differentially and corrected for extinction with nightly extinction coefficients and transformed to the Strömgren system with yearly mean transformation coefficients. A complete discussion of the operation of this telescope and the reduction of the resulting data can be found in Henry (1999). In this paper, we have analyzed data on κ^1 Cet and χ^1 Ori acquired from 2000 November to 2001 January, i.e., contemporaneous with the spectroscopic observations.

2.3. Spectroscopy

Spectroscopic observations were performed in 2000 and 2001 at the M. G. Fracastoro station (Serra La Nave, Mount Etna) of Catania Astrophysical Observatory with FRESCO (Fiber optic REOSC Echelle Spectrograph of Catania Observatory). The echelle spectrograph is connected to the 0.91 m telescope through a fiber link. The spectral resolution was $R = \lambda/\Delta\lambda \simeq 14,000$, with a 2.6 pixel sampling. The data reduction was performed with the ECHELLE task of the IRAF² package following the standard steps: background subtraction, division by a flat-field spectrum from a halogen lamp, wavelength calibration using the emission lines of a Th-Ar lamp, and normalization to the continuum through a poly-

nomial fit. Further details about the instrumentation and data reduction can be found in Catalano et al. (2002).

Our spectra include the H α λ 6563 and He I λ 5876 lines and a number of photospheric lines used for the temperature determination described in § 3.

3. TEMPERATURE AND H α /He I ANALYSIS

Temperature determinations of our target stars have been obtained by measuring the depth ratio of several line pairs, following a method described by Catalano et al. (2002). The line-depth ratios (LDRs) allow us to resolve temperature variations as small as 10 K (Gray & Johanson 1991; Gray & Brown 2001), and the precision improves when one considers the average of several line pairs. For example, Catalano et al. (2002) have demonstrated that LDRs can be used to detect the rotational modulation of the disk-averaged stellar temperature caused by the passage of cool spots across the photospheric disks of active RS CVn stars.

The H α line has proven to be a very good diagnostic of stellar chromospheric activity and is easily accessible at optical wavelengths. Consequently, we have extracted the excess emission in the H α line that, in mildly active stars, partially fills the core of the H α absorption profile. The emission contribution has been extracted with the “spectral synthesis” method (Barden 1985). High signal-to-noise ratio (S/N) spectra of standard stars with negligible activity have been used as inactive templates for the spectral subtraction (see Table 1). The convolution of the template spectra with a proper rotational profile to mimic the $v \sin i$ of each target was not necessary, because the stars analyzed in this paper have rotational velocities lower than 7 km s⁻¹, which is about the FRESCO resolution.

As an additional diagnostic of the upper chromosphere, we have used the He I λ 5876 line, which is seen as an absorption feature in the residual spectra.

3.1. χ^1 Ori = HD 39587

χ^1 Ori ($V = 4.41$ mag) is a MS star that was first detected as an astrometric binary by Lippincott & Worth (1978) and then discovered to be a long-period SB1 ($P_{\text{orb}} = 5156.7$ days) by Han & Gatewood (2002). However, the presence of a low-mass companion in such a wide system should not affect the activity pattern

TABLE 2
SUMMARY OF OBSERVATIONS

HD Number	Spectral Data Range (JD - 2,400,000)	$N_{\text{obs}}^{\text{spectr}}$	Photometric Data Range (JD - 2,400,000)	$N_{\text{obs}}^{\text{photom}}$
166.....	51,834.4–51,865.4	9
20630.....	51,856.5–51,866.5	10	51,810.0–51,975.6	44
22049.....	51,856.5–51,917.4	13
39587.....	51,913.4–51,867.6	14	51,857.9–51,913.7	24

² IRAF is distributed by the National Optical Astronomy Observatory, which is operated by the Association of the Universities for Research in Astronomy, Inc. (AURA), under cooperative agreement with the National Science Foundation.

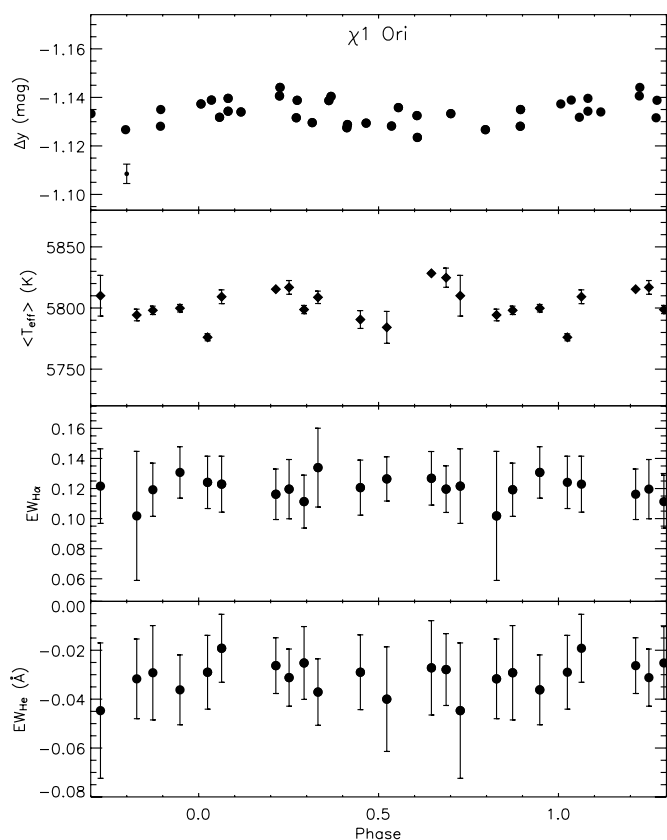


FIG. 1.—From top to bottom: Differential Strömgren y -photometry, $\langle T_{\text{eff}} \rangle$, $EW_{\text{H}\alpha}$, and EW_{He} , all plotted as a function of the rotational phase for χ^1 Ori.

of χ^1 Ori. From a long-term Ca II H and K chromospheric emission analysis, Baliunas et al. (1995) observed significant variability but no clear period. The star is a relatively rapid rotator, since it is a young star belonging to the Ursa Major Cluster with an age of about 300 Myr. König et al. (2002) find $M_1 = 1.01$ and $M_2 = 0.15 M_{\odot}$ from an H -band image of the secondary component taken with the Keck adaptive optics system. The He I line was observed in χ^1 Ori A in absorption by Lambert & O'Brien (1983).

Contemporaneous temperature, light, and $H\alpha$ emission curves of this magnetically active star are plotted in Figure 1. The data have been folded in phase with the ephemeris $\text{HJD}_{\phi=0} = 2,451,856.0 + 5.24E$, where the initial epoch is the date of the first observation and the rotational period is from Messina et al. (2001). The Δy photometry shows a low-amplitude modulation of ~ 0.02 mag. However, neither the net $H\alpha$ equivalent width nor the derived temperature of χ^1 Ori appear to exhibit rotational modulation (Fig. 1). The maximum derived temperature is 5830 K, which is close to the value of 5838 K in Gray (1994), found by means of spectral line-depth ratios from high-resolution spectra.

Spectra of the $H\alpha$ line of all four stars in our sample are shown in Figure 2. The $H\alpha$ profile in χ^1 Ori and the other three stars is always partially filled in by emission. Since χ^1 Ori is a rather active star, as denoted by its excess $H\alpha$ emission, it may be that the lack of rotational modulation in temperature and $H\alpha$ emission is due to observations that were acquired at an epoch of relatively low activity or at a time when the active regions were evenly distributed in longitude. This could also explain the very low amplitude of the light curve.

The He I line is also detected as an absorption feature in the spectra of χ^1 Ori with values of equivalent width around 30 mÅ,

but it does not show a modulation with the phase. Lambert & O'Brien (1983) find a value of $EW_{\text{He}} = 29$ mÅ, and Danks & Lambert (1985) obtain $EW_{\text{He}} = 25$ mÅ, i.e., very close to the equivalent width measured in this work.

3.2. κ^1 Cet = HD 20630

κ^1 Cet ($V = 4.83$ mag) is a nearby (9.16 pc) single G5 dwarf. Evidence of rotational modulation of Ca II H and K chromospheric emission has been found by Vaughan et al. (1981). Changes in its photometric (rotational) period suggest a combination of differential rotation and concentration of starspots at different stellar latitudes from year to year (Gaidos et al. 2000), consistent with a latitude drift of starspots during an activity cycle. In fact, Messina & Guinan (2002) find the existence of a solar-like starspot cycle of 5.9 yr, which is similar to the chromospheric activity cycle of 5.6 yr found by Baliunas et al. (1995). Güdel et al. (1997) estimated an age of 750 Myr for κ^1 Cet from the relatively rapid rotation period of 9.2 days seen in the spot modulation and suggested that the star is a likely member of the Hyades moving group. The He I line was observed in absorption by Lambert & O'Brien (1983), and its equivalent width in the 17.4–25.8 mÅ range appeared rotationally modulated.

The temperature variation derived from our spectra is shown in Figure 3, together with the contemporaneous light curve. The rotational phases have been computed from the ephemeris $\text{HJD}_{\phi=0} = 2,451,856.0 + 9.20E$, where the initial epoch is the date of the first observation and the mean rotational period is from Gaidos et al. (2000). The two curves correlate fairly well, each with a minimum around $\phi \simeq 0.15$ periods and a maximum near $\phi \simeq 0.65$ periods. The amplitude of the temperature curve is about 40 K, with an average value of ~ 5730 K, close to the values of 5718 and 5747 K measured by Gray (1994) and Gaidos & Gonzales (2002) by means of spectroscopic analyses. The light curve has an amplitude of about 0.04 mag.

A spectrum of κ^1 Cet in the $H\alpha$ region is shown in Figure 2. The core of the $H\alpha$ profile is always slightly filled in by emission. The net equivalent width, as measured in the residual spectra, and the average temperature values are plotted in Figure 3. An anticorrelation between the light curve and $EW_{\text{H}\alpha}$ modulation is apparent with the $H\alpha$ minimum at $\phi \simeq 0.65$ periods and the $H\alpha$ maximum near $\phi = 0.15$ periods, i.e., at the same rotational phases as the maximum and the minimum of the light and temperature curves, respectively. This implies a strong spatial correlation between the stellar spots and the chromospheric plagues.

The residual $H\alpha$ profile of κ^1 Cet is relatively narrow ($\text{FWHM} = 0.80\text{--}1.06$ Å) and does not display the broad wings or asymmetric shapes observed in very active RS CVn stars. This implies that the chromospheric active regions in this solar-type star, which is more active than the Sun, nonetheless have a structure similar to the solar plagues and lack the strong mass motions and broadening effects observed in many of the more active RS CVn stars (Hatzes 1995; Biazzo et al. 2006).

The He I line is always observed as an absorption feature whose intensity varies slightly. The large relative errors prevent us from reliably establishing any correlation with the rotational period. The average value of our EW_{He} is about 70 mÅ, i.e., higher than previous results obtained by several authors (Lambert & O'Brien 1983; Danks & Lambert 1985; Saar et al. 1997).

3.3. HD 166

HD 166 ($V = 6.13$ mag) is a nearby (13.7 pc) young solar-type star belonging to the Local Association, a young moving group with stars in an age range from about 50 to 150 Myr (Montes et al. 2001). HD 166 was first found to be a variable star by Rufener &

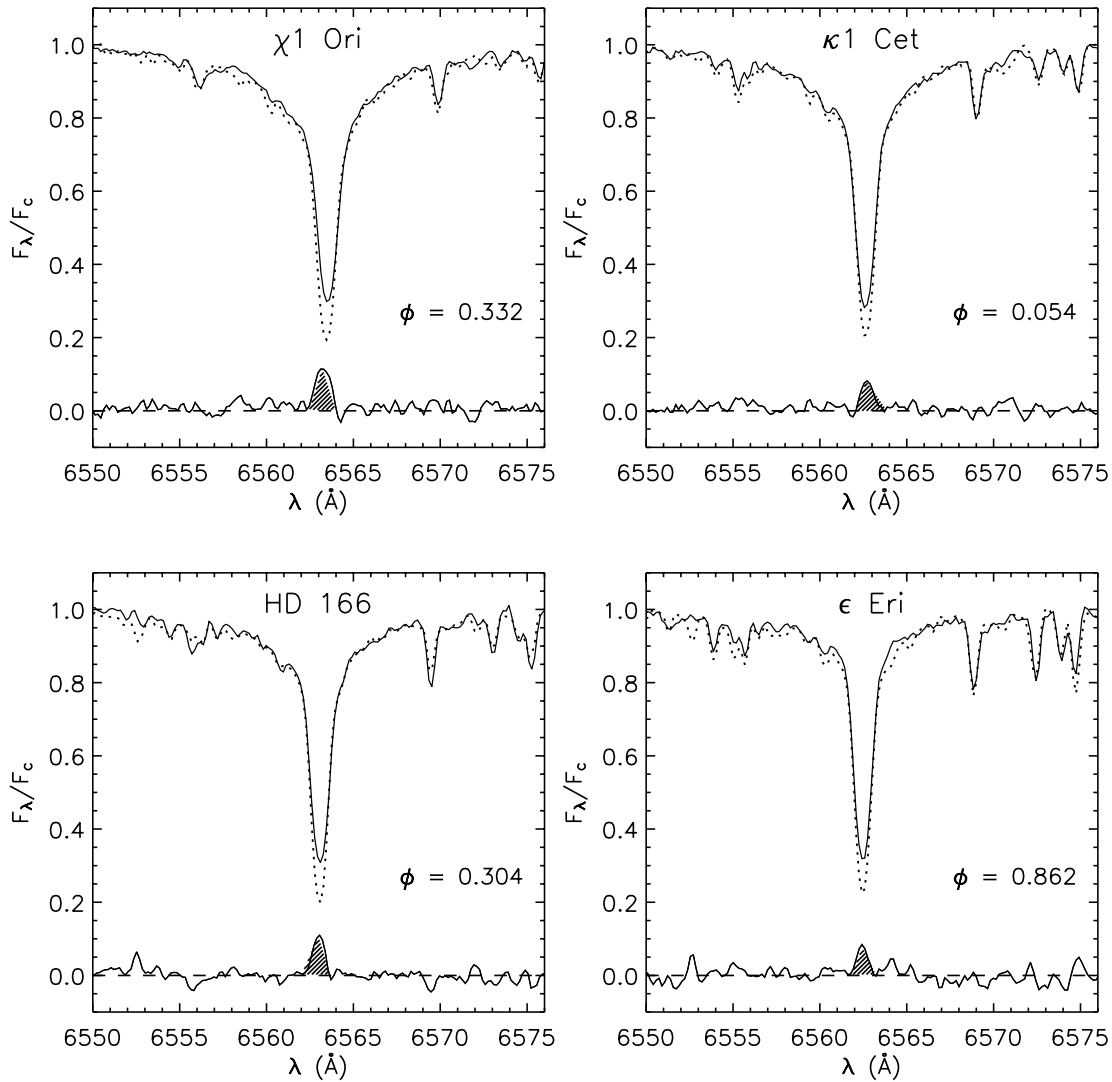


FIG. 2.—Upper part of each panel shows the observed, continuum-normalized spectra of the target stars (*solid line*) in the $H\alpha$ region, together with the inactive stellar template (*dotted line*). Bottom of each panel shows the difference spectra of the two upper spectra.

Bartholdi (1982), who observed “microvariability” in the star’s V magnitudes. New photometric observations were presented by Gaidos et al. (2000); they found the star to vary with an amplitude up to 0.04 mag with a period of 6.23 days. The He I line was observed in absorption by Saar et al. (1997).

Figure 4 plots the temperatures derived from the LDRs in FRESKO spectra as a function of the rotational phase, where the ephemeris used is from Gaidos et al. (2000): $\text{HJD}_{\phi=0} = 2,449,540.0 + 6.23E$. HD 166 shows a clear rotational modulation of the average temperature with an amplitude of about 50 K and a maximum of 5620 K, equal to the value found spectroscopically by Gaidos & Gonzales (2002). Unfortunately, for this star no simultaneous light curve is available.

The variation in the $\text{EW}_{H\alpha}$ is also plotted as a function of the rotational phase in the same figure. We used τ Cet, one of the stars with the lowest level of activity ever observed, as our template star. Notwithstanding the scatter in the $\text{EW}_{H\alpha}$ data, an anticorrelation between photospheric and chromospheric diagnostics is visible. A spectrum of HD 166 in the $H\alpha$ region is presented in Figure 2, where the filling in is evident.

The He I equivalent width that we find has an average value of about 28 mÅ, which is close to the value of 20 mÅ obtained by Saar et al. (1997).

3.4. ϵ Eri = HD 22049

ϵ Eri ($V = 3.73$ mag) is a bright, nearby (3.3 pc) single K2 MS star that shows variability attributed to magnetic activity. From LDR analysis, Gray & Baliunas (1995) find a temperature excursion of about 15 K during the 1986–1992 time interval with rising temperatures associated with higher levels of magnetic activity in the cycle. Long-term photometry has been acquired by Frey et al. (1991) and has led to the detection of a variable rotational period 10.0 days $< P_{\text{rot}} < 12.3$ days, indicative of latitude drift of starspots and differential rotation. Baliunas et al. (1995) measure the Ca II H and K chromospheric emission and report a significant variability with no clear period from the power spectrum analysis. Moreover, the He I line was observed in absorption by Lambert & O’Brien (1983) with no rotational modulation. In a very recent work, Croll et al. (2006) present and analyze high-precision photometry taken with the *MOST* spacecraft during three consecutive rotations of the star. They find evidence of differential rotation with two spots at different latitudes rotating at 11.35 and 11.55 days.

Contemporaneous photometric data are not available for this star; thus, only the analysis of the temperature variations has been done, as shown in Figure 5. Phases have been computed from the

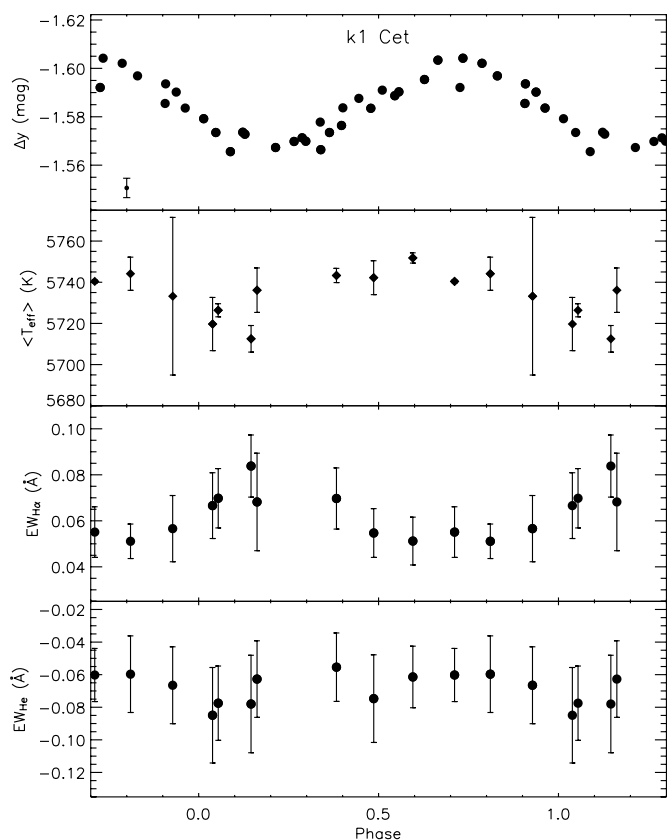


FIG. 3.—From top to bottom: Differential Strömgren γ -photometry, $\langle T_{\text{eff}} \rangle$, $EW_{\text{H}\alpha}$, and EW_{He} as a function of the rotational phase for κ^1 Cet.

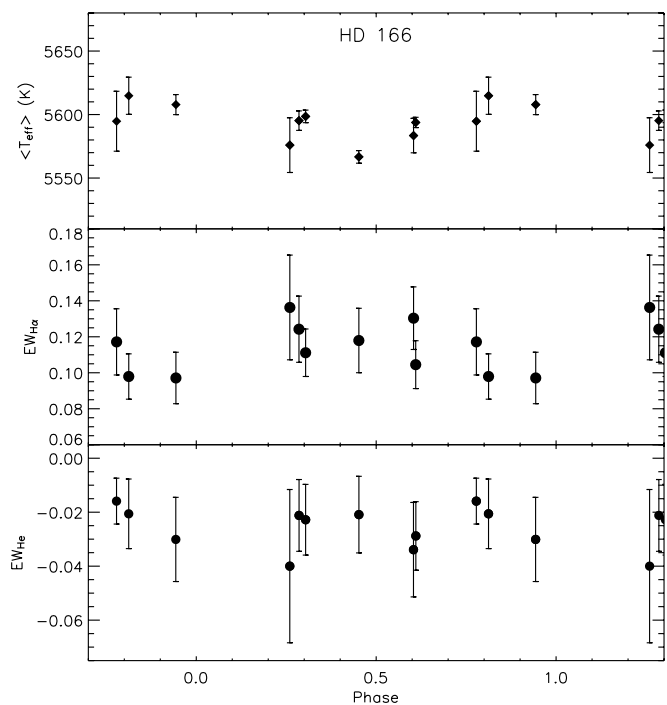


FIG. 4.—From top to bottom: $\langle T_{\text{eff}} \rangle$, $EW_{\text{H}\alpha}$, and EW_{He} as a function of the rotational phase for HD 166.

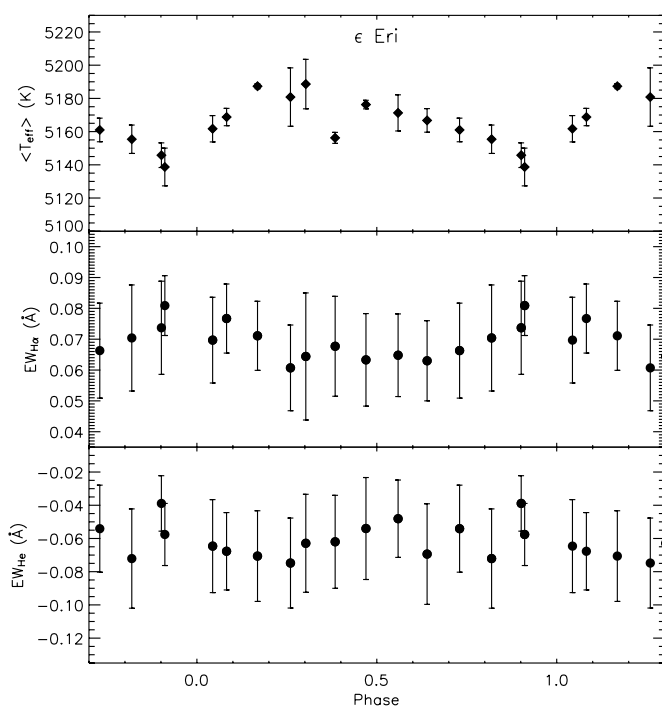


FIG. 5.—From top to bottom: $\langle T_{\text{eff}} \rangle$, $EW_{\text{H}\alpha}$, and EW_{He} as a function of the rotational phase for ϵ Eri.

ephemeris $\text{HJD}_{\phi=0} = 2,451,856.0 + 11.68E$, where the initial epoch is again the date of the first observation and the rotation period is from the analysis of long-term chromospheric activity by Donahue et al. (1996) at Mount Wilson. A clear modulation of the disk-averaged temperature with rotational phase is apparent (Fig. 5). The average T_{eff} value (5160 K) is not far from the value of 5146 K found by Gray (1994) by means of spectral LDRs analysis.

A spectrum of ϵ Eri in the $\text{H}\alpha$ region is shown in Figure 2, while the middle panel of Figure 5 shows the results of the $\text{H}\alpha$ analysis. A fairly well-defined anticorrelation is evident between the photospheric temperature curve and the net $\text{H}\alpha$ equivalent width curve. The full amplitude of the temperature variation is 50 K, i.e., about 1%, while the net $\text{H}\alpha$ equivalent width excursion is about 33% of its average value.

The He I line is also observed in absorption in the spectra of ϵ Eri with values of the disk-averaged equivalent width of about 55 mÅ, but it does not appear to be rotationally modulated. Lambert & O'Brien (1983), Wolf & Heasley (1984), and Danks & Lambert (1985) find values for this parameter in the range 14–18 mÅ.

4. SPOT/PLAGE MODELING

In order to apply our spot model to the observed light and temperature curves, knowledge of geometric and physical parameters of the active stars, such as radius, inclination of the rotation axis with respect to the line of sight, and effective temperature, is required.

The inclination of the rotation axis was estimated through the $v \sin i$, the rotation period, and the stellar radius. The latter was evaluated from the Hipparcos distance and the angular diameter, given by the Barnes & Evans (1976) relation $\log \phi'' = 0.5134 - 0.2V_0 + 0.666(B - V)_0$, where V_0 is the dereddened unspotted magnitude.

To derive the temperature and size of the starspots in a unique way, we have used synthetic light and temperature curves, produced by an appropriate spot model developed by us (Frasca et al.

2005). This model assumes circular dark spots on the surface of a spherical limb-darkened star.

A key parameter for any spot model is the “unspotted” level of the light curve. Analogously, for modeling the temperature curve, one should know the “unperturbed” temperature, i.e., the effective temperature of the stellar photosphere without starspots. However, there is no long-term temperature monitoring of the stars investigated in the present work, so we cannot estimate the “unperturbed” value from the historically recorded maximum, as is frequently done for light-curve modeling. Therefore, we assumed the maximum brightness and temperature observed in our run as the unspotted values. Thus, we are taking into account only the unevenly distributed component of the spotted area, i.e., the component giving rise to the observed rotational modulation. We are possibly underestimating the total spot filling factor, but we are maintaining consistency between the light curve and temperature curve analyses, and we are deducing the starspot parameters for the main active regions causing the modulation.

Since all the observed curves are more or less asymmetric, we modeled two active regions to achieve a satisfactory fit. After several tests, we verified that two spots of the same temperature are sufficient for light-curve fitting with a reasonably low number of free parameters.

The flux ratio between spotted areas and the quiet photosphere, $F_{\text{sp}}/F_{\text{ph}}$, was computed with the low-resolution ATLAS9 synthetic spectra (Kurucz 1993), although the results obtained with the low-resolution PHOENIX NextGen synthetic spectra (Hauschildt et al. 1999) are in good agreement, as already proven by Frasca et al. (2005) for three active evolved stars.

Unfortunately, we could apply the complete analysis only to κ^1 Cet, for which we have contemporaneous spectra and photometry. For the other stars, we have only analyzed the temperature curve, deriving only approximate values of the spot area and temperature.

A rough reconstruction of the chromospheric inhomogeneities has been also derived by applying a simple plage model to the $H\alpha$ rotational modulation. The model assumes two bright circular plages (Frasca et al. 2000) with an emission flux ratio (with respect to the quiet chromosphere) $F_{\text{plage}}/F_{\text{chrom}} = 3$, which is typical of the brightest $H\alpha$ solar plages. A lower contrast produces a slightly worse fit of the $H\alpha$ curves, along with larger plages. The solutions provide the longitude of the plages but give only rough estimates of their latitude and size. The latter parameter is strongly dependent on the assumed flux contrast $F_{\text{plage}}/F_{\text{chrom}}$. Therefore, only the combined effects of plage dimensions and flux contrast, a sort of plage luminosity in the $H\alpha$ line, in units of the quiet chromosphere, can be derived. Furthermore, we point out that we do not know the quiet chromospheric (network) contribution, since the $H\alpha$ minimum value (EW_{chrom}) could be still affected by a homogeneous distribution of small plages.

4.1. κ^1 Cet

The assumed temperature of the quiet photosphere, determined from the maximum of the $\langle T_{\text{eff}} \rangle$ curve, is $T_{\text{ph}} \simeq 5750$ K. This is obviously a lower limit, since we cannot exclude the presence of polar caps or a uniform distribution of small starspots, i.e., those features that do not produce any light or temperature modulation but that slightly affect the stellar spectrum at the phase of minimum visibility of the two main starspots.

From the unspotted magnitude, $V_{\text{max}} = 4.80$ mag (Messina & Guinan 2002), and color index, $(B - V) = 0.680$ mag (Gonzalez & Piche 1992), the stellar radius derived for κ^1 Cet is $R_1 = 1.00 R_{\odot}$. The inclination derived from this value of the radius,

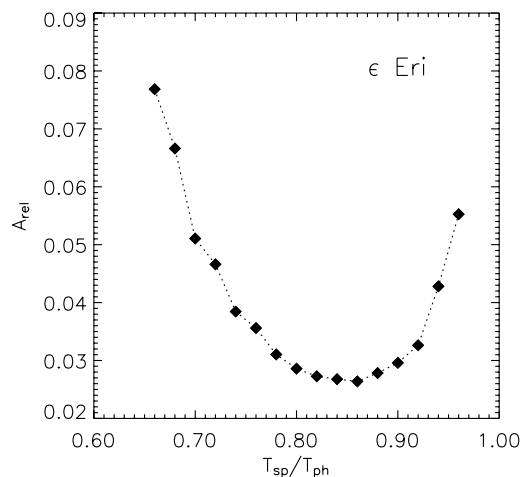
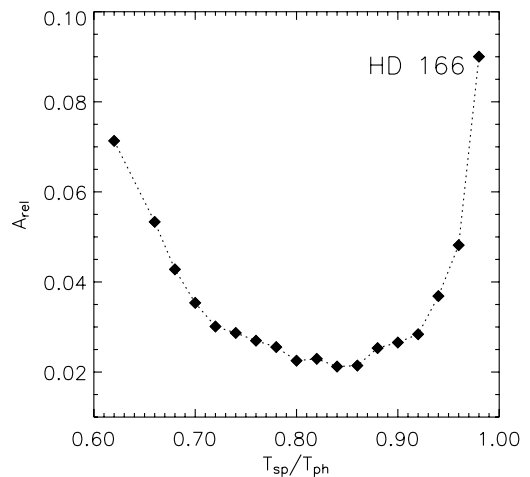
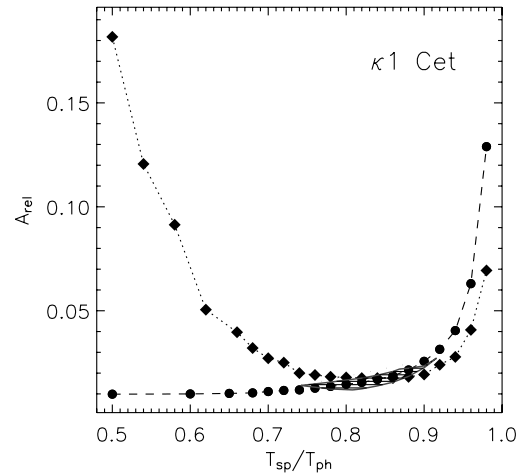


FIG. 6.—*Top*: Grids of solutions for κ^1 Cet. The circles represent the solutions for light curve, while the diamonds represent the solutions for temperature curve. The hatched area is the locus of the allowed solutions accounting for data errors. *Middle*: Grid of solutions for the temperature curve of HD 166. *Bottom*: Grid of solutions for the temperature curve of ϵ Eri.

$v \sin i = 4.5 \text{ km s}^{-1}$, and $P_{\text{rot}} = 9.2$ days (Gaidos et al. 2000) is $i = 55^{+28}_{-14}$ deg. Rucinski et al. (2004) measured a value of $v \sin i = 4.64 \pm 0.11 \text{ km s}^{-1}$, in good agreement with the Gaidos et al. (2000) determination, and deduced an inclination of $i = 60^\circ \pm 5^\circ$, close to our own value. The same authors also derived a

TABLE 3
SPOT/PLAGE CONFIGURATION FOR κ^1 CET, HD 166, AND ϵ ERI

Radius (deg)	Longitude ^a (deg)	Latitude (deg)	$T_{\text{sp}}/T_{\text{ph}}$	T_{ph} (K)	T_{sp} (K)	$A_{\text{rel}}^{\text{b}}$
κ^1 Cet ($\mu_y = 0.669$, $\mu_{6200} = 0.56$, $\text{EW}_{\text{chrom}} = 0.051 \text{ \AA}$)						
Spots:						
12.2.....	30	38	$0.85^{+0.07}_{-0.10}$	5750	4890^{+390}_{-600}	$0.018^{+0.009}_{-0.006}$
9.0.....	130	28
Plages:						
24.8.....	30	38	0.074
19.3.....	130	28
HD 166 ($\mu_{6200} = 0.56$, $\text{EW}_{\text{chrom}} = 0.097 \text{ \AA}$)						
Spots:						
14.1.....	153	46	0.84	5620	4720	0.021
9.0.....	204	20
Plages:						
20.5.....	152	47	0.047
14.2.....	201	24
ϵ Eri ($\mu_{6200} = 0.59$, $\text{EW}_{\text{chrom}} = 0.061 \text{ \AA}$)						
Spots:						
16.3.....	298	48	0.86	5190	4460	0.026
9.1.....	348	21
Plages:						
17.8.....	326	46	0.034
11.6.....	5	21

^a Longitude increases with phase, and 0° longitude corresponds to phase 0.0 periods.

^b Total fractional area of the two spots.

value of $i = 70^\circ \pm 4^\circ$ by leaving the inclination as an adjustable parameter in their spot model.

We find two grids of solutions for the Δy and $\langle T_{\text{eff}} \rangle$ curves, whose unique intersection provides the best values of the spot temperature T_{sp} and the projected area of the spots relative to the stellar surface A_{rel} (Fig. 6). By fixing $i = 55^\circ$, we find a relative spot temperature $T_{\text{sp}}/T_{\text{ph}} = 0.85$ and a relative spot area $A_{\text{rel}} = 0.018$. If we assume the Rucinski et al. (2004) value for the inclination ($i = 70^\circ$), the temperature and area deduced from the spot modeling undergo only marginal changes ($T_{\text{sp}}/T_{\text{ph}} = 0.82$, $A_{\text{rel}} = 0.017$), with spots only 4% cooler and a total spotted area 6% smaller. Our derived radii for the two spots are 12° and 9° , very close to the values found by Rucinski et al. (2004) from their very accurate light curve obtained with the *MOST* satellite.

For the $\text{H}\alpha$ curve, we applied a simple plage model with two bright plages (Frasca et al. 2000). We fixed the emission flux ratio between plages and quiet chromosphere $F_{\text{plage}}/F_{\text{chrom}} = 3$, typical of the brightest solar plages.

In Table 3, our derived spot/plage configuration is reported, where μ_y and μ_{6200} are the linear limb-darkening coefficients for the y band and for the continuum at 6250 \AA . EW_{chrom} is the value of the $\text{H}\alpha$ equivalent width at the minimum of the rotational modulation.

The photospheric and chromospheric active regions have no appreciable longitude shifts (Table 3; Fig. 7). This result is similar to that obtained by Frasca et al. (2000) for the young solar-type star HD 206860.

4.2. HD 166 and ϵ Eri

For HD 166 and ϵ Eri we have no photometric data contemporaneous to the spectroscopic observations. As a consequence, we have applied the spot modeling only to the temperature curve,

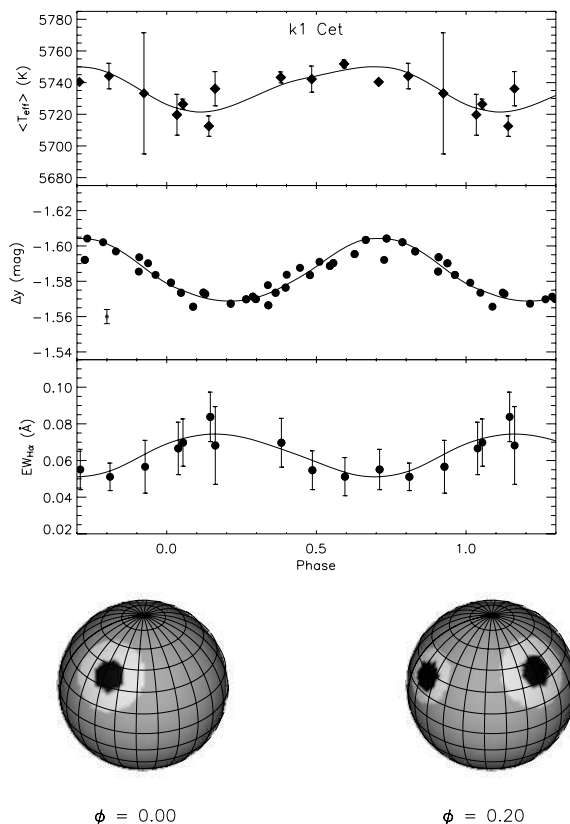


FIG. 7.—Observed (filled circles) and synthetic (solid lines) temperature, light, and $\text{EW}_{\text{H}\alpha}$ curves of κ^1 Cet. The solutions are those obtained with the Kurucz model (Kurucz 1993).

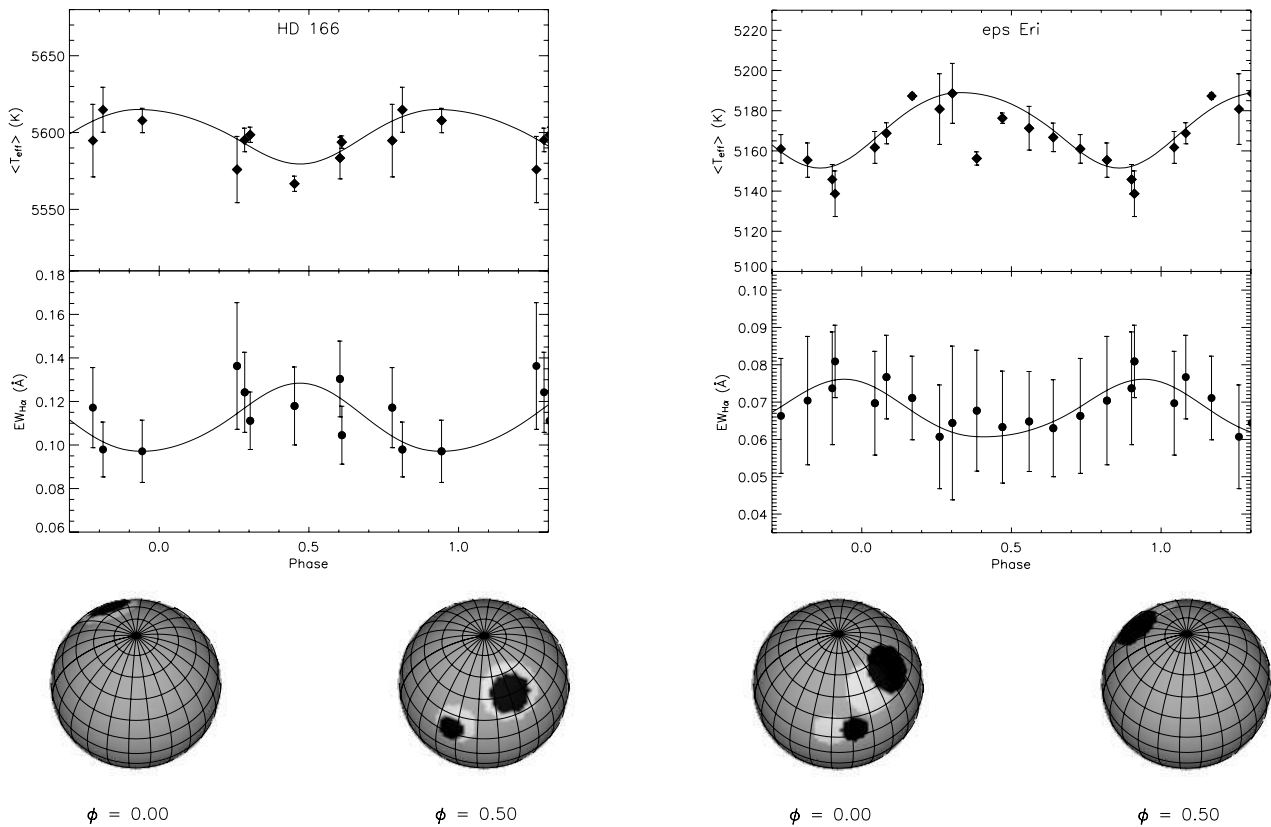


Fig. 8.—Observed (filled diamonds and circles) and synthetic (solid lines) temperature and $EW_{H\alpha}$ curves of HD 166 and ϵ Eri.

obtaining the minima of the temperature grids for $A_{\text{rel}} = 0.021$ and 0.026 , which correspond to $T_{\text{sp}}/T_{\text{ph}} = 0.84$ and 0.86 for HD 166 and ϵ Eri, respectively (Fig. 6).

The inclination of the rotation axis found by us for ϵ Eri is of $\simeq 30^\circ$ (Table 1), in very good agreement with the values found by Hatzes et al. (2000) and Croll et al. (2006), and $i \approx 25^\circ$ derived by Greaves et al. (2005) for the debris disk. For HD 166 we found $i = 34^\circ$.

In Table 3 we list the approximate values of the spot solutions. These values are listed without error bars because it is impossible with only the temperature curve to define the locus of the allowed solutions. Because in the cases of κ^1 Cet presented here and of the RS CVn binaries analyzed by Frasca et al. (2005) the unique spot solution obtained from the intersection of the two light and temperature grids is near the minimum of the grid of solutions for the temperature curve, we assume that, for HD 166 and ϵ Eri, the unique solution is near the temperature grid minima of $T_{\text{sp}}/T_{\text{ph}} = 0.84$ and 0.86 , respectively. The high-precision light curve obtained with the *MOST* spacecraft in the fall of 2005, covering three stellar rotations, has been analyzed by Croll et al. (2006). Their spot model provides a best-fit solution with two circular spots with angular radii of about 7° , with a fixed flux ratio of 0.22 , corresponding to a temperature factor of about 0.7 at the central wavelength of the *MOST* passband, i.e., they assume spots that are considerably cooler compared to ours. However, their observations were taken with a single very broad filter ($3500\text{--}7000 \text{ \AA}$), which prevents them from deriving the spot temperatures. A spot temperature equal to ours would result in somewhat larger spots, in closer agreement with our results.

Finally, the simple plage model described by Frasca et al. (2000) has been applied to these two stars, fixing $F_{\text{plage}}/F_{\text{chrom}} = 3$. The derived plage parameters are recorded in Table 3.

The spot/plage configuration of HD 166 and ϵ Eri is displayed in Figure 8.

5. CONCLUSION

We have analyzed the photospheric and chromospheric activity in four young, magnetically active solar-type stars, namely χ^1 Ori, κ^1 Cet, HD 166, and ϵ Eri. The photospheric surface features have been recovered by means of the rotational modulation of luminosity and temperature, as derived from the LDR method, while the chromospheric inhomogeneities have been studied from their excess $H\alpha$ emission. The $H\alpha$ profiles can be reasonably well reproduced by means of only one Gaussian component, indicating the presence of plages spatially associated with the photospheric spots. The temperature and light curves are always anticorrelated with the $H\alpha$ emission modulation, confirming a close spatial association between spots and plages. The only exception is χ^1 Ori, for which we have not obtained clear rotational modulation of temperature and $H\alpha$ curves. The He I D_3 line is always present in our spectra, but the EW_{He} measurements show too much scatter to reveal any modulation with the rotational phase, with the possible exception of κ^1 Cet, for which a marginal modulation is seen. Thus, in general, the active regions in mildly active stars seem to have structures similar to solar active regions.

The spectroscopic measurements of HD 166 and ϵ Eri span about five stellar rotations, but the spot/plage configuration seems to be largely unchanging, as observed in some other young solar analogs in which the light curve remains stable for several rotations (Messina & Guinan 2002).

Moreover, from a simple spot/plage model analysis, we have derived spot and plage parameters (temperature and area). In the case of κ^1 Cet, for which we had both simultaneous photometric

and spectroscopic data, spot temperature and area have been uniquely determined. The grid of the temperature solutions is flat because of the small amplitude of the temperature curve of this MS star; this leads to great errors in the unique spot solution. For HD 166 and ϵ Eri, we have also presented a rough estimate of these two parameters.

Finally, the temperature difference ΔT between the quiet photosphere and spots, a key parameter tied to the blocking effect on convection produced by the intensification of the magnetic field, ranges from 730 to 900 K for the three active stars. Considering the errors, these values are not significantly higher than those derived with the same technique by Frasca et al. (2005) for stars with lower gravity ($\Delta T = 450\text{--}840$ K). However, we need data with higher accuracy and a broader stellar sample to investigate any possible dependency of ΔT on surface gravity.

On the other hand, the dimensions of the spots on κ^1 Cet, HD 166, and ϵ Eri are significantly smaller than those on the three very active stars studied by Frasca et al. (2005). It is not yet clear whether this is merely the effect of the lower activity level of the young stars studied in the present work compared to the very active RS CVn stars investigated by Frasca et al. (2005), or whether the stellar temperature and/or gravity are responsible for the different spot dimensions.

Moreover, with the assumed value of the flux contrast, $F_{\text{plage}}/F_{\text{chrom}} = 3$, the chromospheric plages are larger than the associated spots, as usually observed in the Sun. As a consequence, the increasing dissipation of magnetic energy with height above the photosphere seems to occur for these solar-type stars as well. For the evolved stars investigated by Frasca et al. (2005) and Biazzo et al. (2006), there is an indication that plage areas are larger still and closer to the spot areas. In future studies, we want first to extend the number of main sequence targets and then investigate the inhomogeneities at photospheric and chromospheric levels in pre-main-sequence, rapidly rotating stars to separate gravitational effects from activity level.

We thank Katalin Oláh for the excellent suggestions, which helped us to improve the quality and consistency of the paper. This work has been supported by the Italian Ministero dell'Istruzione, Università e Ricerca (MIUR) and by the Regione Sicilia, which are gratefully acknowledged. G. W. H. acknowledges support from NASA grant NCC5-511 and NSF grant HRD-9550561. This research has also made use of the SIMBAD and VIZIER databases, operated at CDS, Strasbourg, France.

REFERENCES

- Baliunas, S. L., et al. 1995, *ApJ*, 438, 269
 Barden, S. C. 1985, *ApJ*, 295, 162
 Barnes, T. G., & Evans, D. S. 1976, *MNRAS*, 174, 489
 Biazzo, K., Frasca, A., Catalano, S., & Marilli, E. 2006, *A&A*, 446, 1129
 Catalano, S., Biazzo, K., Frasca, A., & Marilli, E. 2002, *A&A*, 394, 1009
 Croll, B., et al. 2006, *ApJ*, 648, 607
 Danks, A. C., & Lambert, D. L. 1985, *A&A*, 148, 293
 Donahue, R. A., Saar, S. H., & Baliunas, S. L. 1996, *ApJ*, 466, 384
 Fekel, F. C. 1997, *PASP*, 109, 514
 Frasca, A., Biazzo, K., Catalano, S., Marilli, E., Messina, S., & Rodonò, M. 2005, *A&A*, 432, 647
 Frasca, A., & Catalano, S. 1994, *A&A*, 284, 883
 Frasca, A., Catalano, S., & Mantovani, D. 1997, *A&A*, 320, 101
 Frasca, A., Freire Ferrero, R., Marilli, E., & Catalano, S. 2000, *A&A*, 364, 179
 Frey, G. J., et al. 1991, *AJ*, 102, 1813
 Gaidos, E. J., & Gonzales, G. 2002, *NewA*, 7, 211
 Gaidos, E. J., Henry, G. W., & Henry, S. M. 2000, *AJ*, 120, 1006
 Gonzalez, G., & Piche, F. 1992, *AJ*, 103, 2048
 Gray, D. F. 1994, *PASP*, 106, 1248
 Gray, D. F., & Baliunas, S. L. 1995, *ApJ*, 441, 436
 Gray, D. F., & Brown, K. 2001, *PASP*, 113, 723
 Gray, D. F., & Johanson, H. L. 1991, *PASP*, 103, 439
 Greaves, J. S., et al. 2005, *ApJ*, 619, L187
 Güdel, M., Guinan, E. F., & Skinner, S. L. 1997, *ApJ*, 483, 947
 Han, I., & Gatewood, G. 2002, *PASP*, 114, 224
 Hatzes, A. P. 1995, *AJ*, 109, 350
 Hatzes, A. P., et al. 2000, *ApJ*, 544, L145
 Hauschildt, P. H., Allard, F., & Baron, E. 1999, *ApJ*, 512, 377
 Henry, G. W. 1999, *PASP*, 111, 845
 Johnson, H. L., Iriarte, B., Mitchell, R. I., & Wisniewski, W. Z. 1966, *Comm. Lunar Planet. Lab.*, 4, 99
 König, B., et al. 2002, *A&A*, 394, L43
 Kurucz, R. L. 1993, Kurucz CD-ROM 13, ATLAS9 Stellar Atmosphere Programs and 2 km s⁻¹ Grid (Cambridge: SAO)
 Lambert, D. L., & O'Brien, G. T. 1983, *A&A*, 128, 110
 Lippincott, S. L., & Worth, M. D. 1978, *PASP*, 90, 330
 Lockwood, G. W., Skiff, B. A., & Radick, R. R. 1997, *ApJ*, 485, 789
 Messina, S., & Guinan, E. F. 2002, *A&A*, 393, 225
 Messina, S., Rodonò, M., & Guinan, E. F. 2001, *A&A*, 366, 215
 Montes, D., López-Santiago, J., Gálvez, M. C., Fernández-Figueroa, M. J., De Castro, E., & Cornide, M. 2001, *MNRAS*, 328, 45
 Radick, R. R., Lockwood, G. W., Skiff, B. A., & Baliunas, S. L. 1998, *ApJS*, 118, 239
 Radick, R. R., et al. 1983, *PASP*, 95, 300
 Rucinski, S. M., et al. 2004, *PASP*, 116, 1093
 Rufener, F., & Bartholdi, P. 1982, *A&AS*, 48, 503
 Saar, S. H., Huovelin, J., Osten, R. A., & Shcherbakov, A. G. 1997, *A&A*, 326, 741
 Saar, S. H., & Osten, R. A. 1997, *MNRAS*, 284, 803
 Stout-Batalha, N. M., & Vogt, S. S. 1999, *ApJS*, 123, 251
 Strassmeier, K. G., Rice, J. B., Wehlau, W. H., Hill, G. M., & Matthews, J. M. 1993, *A&A*, 268, 671
 Vaughan, A. H., et al. 1981, *ApJ*, 250, 276
 Wolff, S. C., & Heasley, J. N. 1984, *PASP*, 96, 231